

Peptidoglycan recycling mediated by an ABC transporter in the plant pathogen *Agrobacterium tumefaciens*

Received: 9 August 2022

Accepted: 13 December 2022

Published online: 24 December 2022

 Check for updatesMichael C. Gilmore¹ & Felipe Cava¹ ✉

During growth and division, the bacterial cell wall peptidoglycan (PG) is remodelled, resulting in the liberation of PG muropeptides which are typically reinternalized and recycled. Bacteria belonging to the Rhizobiales and Rhodobacterales orders of the Alphaproteobacteria lack the muropeptide transporter AmpG, despite having other key PG recycling enzymes. Here, we show that an alternative transporter, YejBEF-YepA, takes over this role in the Rhizobiales phytopathogen *Agrobacterium tumefaciens*. Muropeptide import by YejBEF-YepA governs expression of the β -lactamase AmpC in *A. tumefaciens*, contributing to β -lactam resistance. However, we show that the absence of YejBEF-YepA causes severe cell wall defects that go far beyond lowered AmpC activity. Thus, contrary to previously established Gram-negative models, PG recycling is vital for cell wall integrity in *A. tumefaciens*. YepA is widespread in the Rhizobiales and Rhodobacterales, suggesting that YejBEF-YepA-mediated PG recycling could represent an important but overlooked aspect of cell wall biology in these bacteria.

The bacterial cell wall is composed primarily of peptidoglycan (PG), a heteropolymer which consists of alternating *N*-acetylglucosamine (GlcNAc) and *N*-acetylmuramic acid (MurNAc) sugars crosslinked by short peptide chains¹. In order to facilitate growth and division, as well as adaption to environmental stressors, the cell wall is constantly remodelled by an arsenal of lytic enzymes²: glucosaminidases and lysozyme cleave between the two sugars, endopeptidases cleave within the peptide chains, carboxypeptidases cleave the C-terminal amino acid from the peptide chains, amidases cleave the peptide chain from the MurNAc sugar and lytic transglycosylases (LTs) cleave between the sugars with simultaneous cyclisation of the terminal MurNAc to form 1,6-anhydroMurNAc. A consequence of this remodelling activity is the liberation of PG fragments, termed muropeptides, which can be released into the environment where they can have far-reaching consequences in signalling or interspecies interactions³, or imported into the cell for reuse in PG synthesis, in a process termed PG recycling⁴.

PG recycling has been well studied in some Gram-negative models. Typically, anhydromuropeptides liberated by LTs are imported by the Major Facilitator Superfamily (MFS) transporter AmpG⁵,

before being broken into their constituent sugars and peptide by the amidase AmpD⁶, β -hexosaminidase NagZ^{7,8} and LD-carboxypeptidase LdcA⁹ (Fig. 1A). Pathways exist for recycling both the anhydroMurNAc and GlcNAc sugars^{4,10–12}, while the peptide is directly reincorporated into PG synthesis by ligation with UDP-MurNAc by the ligase Mpl¹³ ultimately resulting in the production of the primary soluble PG precursor, UDP-muramylpentapeptide (UDP-M5). Around 50% of the sacculus is turned over in *Escherichia coli* per generation¹⁴, but only around 8% is released to the medium, due to recycling¹⁵. Despite the extent of PG turnover, the abundance of proteins produced solely to enable PG recycling and its relatively wide conservation, its importance is unclear, since its interruption does not affect bacterial growth under laboratory conditions⁴. The exception to this is a growth defect caused by the deletion of the LD-carboxypeptidase LdcA, which leads to a reduction in cell wall crosslinking due to the inability of tetrapeptide precursors to be used as a donor in the PG transpeptidation reaction^{9,16}.

We noticed that Alphaproteobacteria belonging to the orders Rhizobiales and Rhodobacterales lack AmpG orthologs, despite

¹Laboratory for Molecular Infection Medicine Sweden (MIMS), Umeå Center for Microbial Research (UCMR), Department of Molecular Biology, Umeå University, 90187 Umeå, Sweden. ✉e-mail: felipe.cava@umu.se

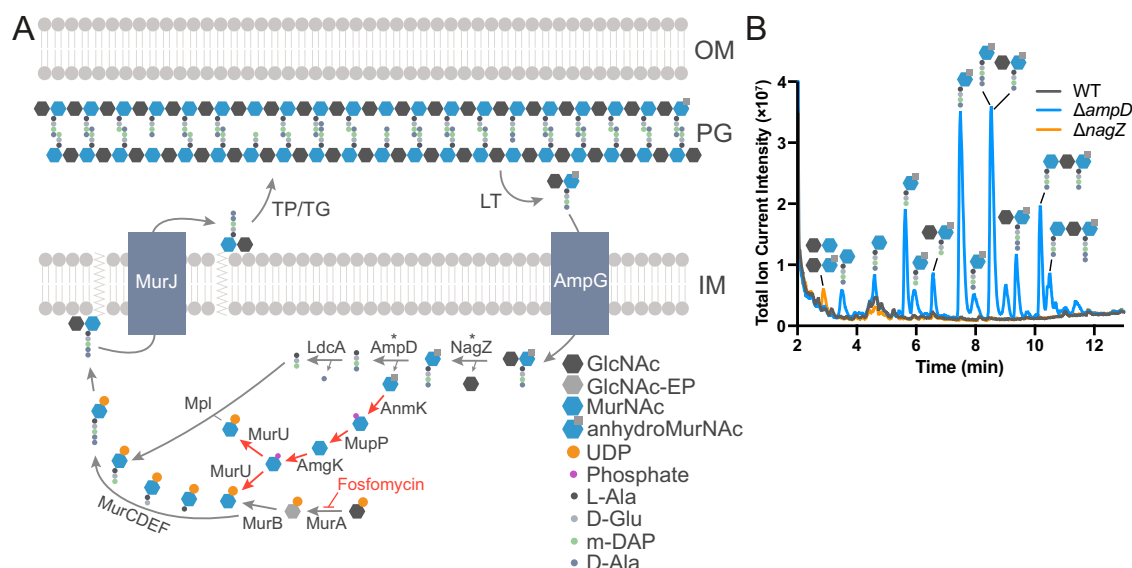


Fig. 1 | *A. tumefaciens* recycles muropeptides. A Schematic diagram of PG recycling pathway in *E. coli*. *Pseudomonas* MurNac recycling pathway depicted with red arrows. EP enolpyruvate, TP transpeptidase, TG transglycosylase, LT lytic transglycosylase, OM outer membrane, PG peptidoglycan, IM inner membrane. * AmpD and NagZ activities are promiscuous: AmpD can act on muropeptides with or

without GlcNAc⁶, and NagZ can act on disaccharides with or without peptide chain^{7,8}. **B** Total Ion Current (TIC) chromatogram showing soluble PG fragments that accumulate in the cytoplasm of *A. tumefaciens* WT, $\Delta ampD$ and $\Delta nagZ$ strains detected using LC-MS.

encoding orthologs of other PG recycling enzymes such as AmpD and NagZ in their genomes. Using the plant pathogen *Agrobacterium tumefaciens* as model, we show that the broad-specificity peptide ABC transporter YejBEF takes over the role of AmpG as muropeptide transporter in these bacteria, utilising an alternative PG-specific substrate-binding protein (SBP) YepA which is unique to the Alphaproteobacteria. PG recycling mediated by YejBEF-YepA governs expression of the β -lactamase AmpC through a canonical AmpR repression system, controlling β -lactam resistance in *A. tumefaciens* in place of AmpG. Importantly, we show that contrary to previously established Gram-negative models, PG recycling is vital for cell wall integrity in this bacterium since deleting the transporter results in significantly altered cell wall density and composition, leading to growth defects on low-osmolarity medium and hypersensitivity to β -lactam antibiotics in a manner partly independent of AmpC.

Results

A. tumefaciens recycles PG

We first set out to determine if *A. tumefaciens* recycles PG, since it lacks an ortholog of the PG recycling transporter AmpG. Since deletion of the anhydromuramylamidase AmpD results in the accumulation of anhydromuramyl tripeptides in the cytoplasm of *E. coli*⁶, we deleted the *A. tumefaciens* orthologs of both *ampD* (Atu2113) and *nagZ* (Atu1709) and used ultra-performance liquid chromatography coupled to quadrupole-time of flight mass spectrometry (UPLC-MS) to check for the accumulation of the substrates of these enzymes in the cytoplasm (Fig. 1B). We observed the accumulation of anhydroMurNac- and MurNac-linked muropeptide species accumulating in the cytoplasm of $\Delta ampD$, while the GlcNAc-anhydroMurNac and GlcNAc-MurNac disaccharides accumulated in the cytoplasm of $\Delta nagZ$, confirming these enzymes play the same respective roles in PG recycling in *A. tumefaciens* as in other Gram-negative bacteria. Interestingly, we observed tri-, tetra- and pentapeptide-containing muropeptides accumulating in $\Delta ampD$. In *E. coli*, typically only tripeptide muropeptides are observed to accumulate in an *ampD* mutant due to the activity of the LD-carboxypeptidase LdcA⁶, suggesting that *A. tumefaciens* lacks this activity in its cytoplasm. To confirm this, we ectopically expressed LdcA from *E. coli* in *A. tumefaciens* on a plasmid

and observed a corresponding shift in accumulation from tetrapeptide to tripeptide muropeptides (Fig. S1). In addition, trisaccharide muropeptides also accumulated in $\Delta ampD$, suggesting that *A. tumefaciens* can transport dimers into its cytoplasm for recycling. The ion masses of these were consistent with either DD-crosslinked dimers or linear (uncrosslinked) chains. The possibility of these being LD-crosslinked was excluded because LD-crosslinked dimers include a tripeptide stem as a result of the LD-transpeptidation reaction¹⁷. LdcA expression allowed us to establish their identity as linear dimers as it resulted in dipeptides (i.e. M3-M3, Fig. S1), instead of the M3 and M4-D-Ala monomers that would be expected from LdcA cleavage of D44, assuming that the crosslinked D-Ala was still usable as a substrate for LdcA. Collectively, these results indicate that *A. tumefaciens* does recycle PG and thus suggested the existence of an alternative transporter of muropeptides, with a slightly altered substrate specificity to AmpG.

Identification of the PG recycling transporter in *A. tumefaciens*

To identify the missing transporter, we took advantage of the antibiotic Fosfomycin. This inhibits the first committed step of PG synthesis, the MurA-catalysed conversion of UDP-GlcNAc into UDP-GlcNAc-enolpyruvate, which forms the substrate for the subsequent production of UDP-MurNac by MurB¹⁸ (Fig. 1A). This step can be bypassed to some extent by the recycling of MurNac, which confers higher intrinsic resistance to Fosfomycin¹⁰. We therefore used a high-throughput transposon sequencing screen (Tn-Seq) to identify genes which are required for survival under Fosfomycin treatment, reasoning that this should reveal genes required for recycling MurNac in *A. tumefaciens*, and thus our transporter. Our Fosfomycin Tn-Seq screen revealed that recycling of MurNac in *A. tumefaciens* likely happens as in *Pseudomonas* spp.^{10–12}, using the enzymes AnmK (Atu1827), MupP (Atu1614), AmgK (Atu0026) and MurU (Atu0025) to process anhydroMurNac and convert it into UDP-MurNac for reuse (Supplementary Data 1). In the list of genes which were statistically underrepresented in transposon insertions with 2 mg/mL Fosfomycin (Fig. 2A, Supplementary Data 1), there were two ATP-binding cassette (ABC) transporters. One consisted of the membrane-spanning and nucleotide-binding proteins of the phosphonate ABC importer *phnJK*, which is reported to form

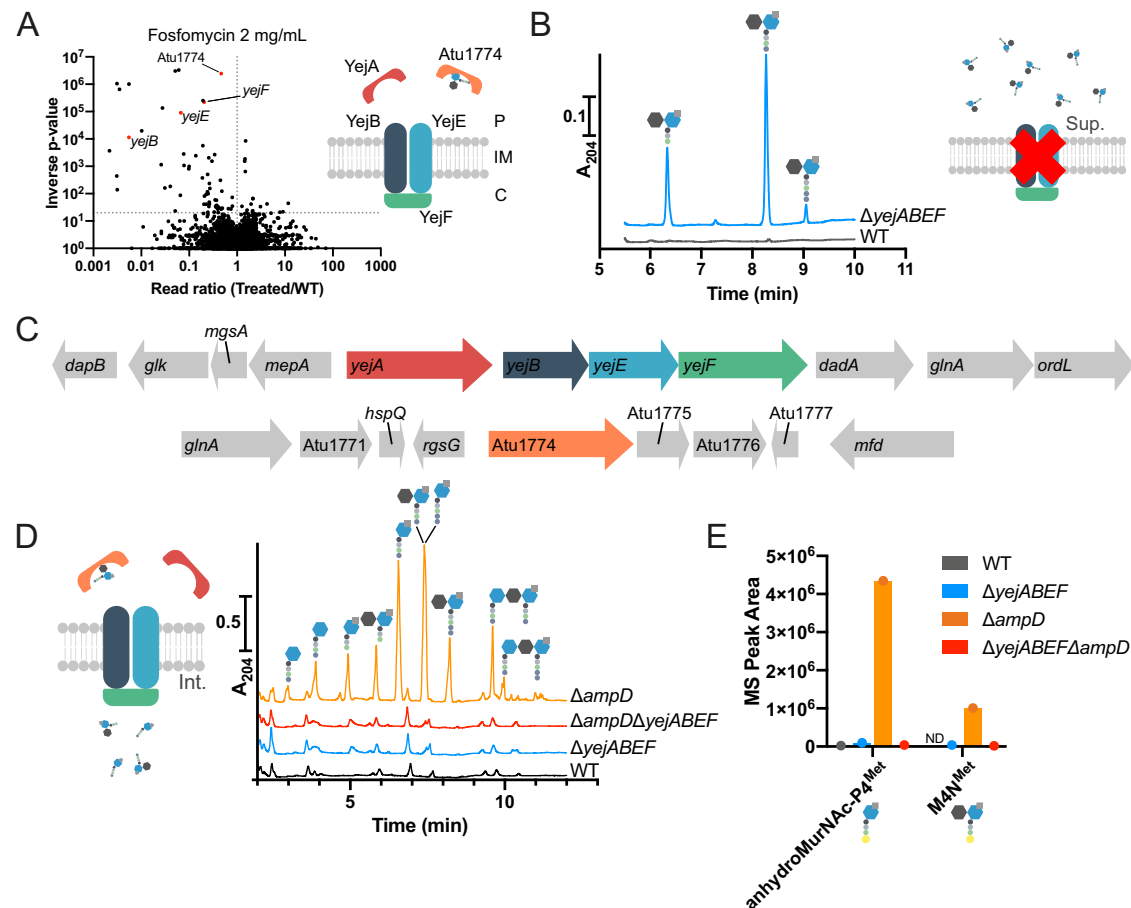


Fig. 2 | YejBEF is the PG recycling transporter in *A. tumefaciens*. **A** Volcano plot showing the ratio of Transposon sequencing (Tn-Seq) reads mapped to genes in the *A. tumefaciens* WT strain treated with 2 mg/mL Fosfomycin compared to control, plotted against inverse p value determined by Mann–Whitney U test (threshold $p^{-1} > 20$). Genes corresponding to *yejBEF* and *Atu1774* are highlighted in the volcano plot in red; their localisation in the schematic is determined by their annotation as periplasmic substrate-binding proteins, membrane-spanning proteins or cytoplasmic ATPase. C, cytoplasm. IM, inner membrane. P, periplasm. **B** UPLC

chromatogram showing levels of anhydromuropeptides released into the supernatants by *A. tumefaciens* WT and $\Delta yejABEF$ strains. Peaks identified using retention time and in-line LC-MS. **C** Genomic context of *yejABEF* and *Atu1774*. **D** Soluble PG fragments that accumulate in *A. tumefaciens* WT, $\Delta yejABEF$, $\Delta ampD$ and $\Delta yejABEF \Delta ampD$ strains detected using UPLC. **E** Quantification of D-Met containing soluble precursors in *A. tumefaciens* WT, $\Delta yejABEF$, $\Delta ampD$ and $\Delta yejABEF \Delta ampD$ strains treated with exogenous M4N^{Met} by LC-MS. ND, not detected. $n = 1$ biological replicate. Source data are provided as a Source Data file.

part of the carbon-phosphorus (C-P) lyase machinery^{19,20}. Since this complex mediates the cleavage of C-P bonds, such as that found in Fosfomycin, it likely confers resistance to Fosfomycin by degrading it. Indeed, degradation of Fosfomycin by Rhizobiales bacteria has been previously observed²¹, and this process could explain the relatively high intrinsic Fosfomycin resistance in *A. tumefaciens*. The other ABC transporter with significantly reduced Tn insertions was a putative peptide ABC importer previously reported as YejBEF (Fig. 2A) consisting of two membrane-spanning proteins *yejB* and *yejE* (Atu0188 and Atu0189) and an ATPase *yejF* (Atu0190). Interestingly, these genes form an operon with a periplasmic SBP, *yejA* (Atu0187) which was not affected in Tn insertions under Fosfomycin treatment. Instead, our screen identified an alternative peptide-binding SBP (Atu1774) with significantly fewer Tn insertions, which showed sequence similarity to *yejA* (38.7% identity). The YejABEF ABC transporter has previously been reported as a broad-specificity peptide importer required for resistance to plant antimicrobial peptides and proper bacteroid differentiation in *Sinorhizobium meliloti*^{22,23}, and thus together with the SBP *Atu1774*, represented a good candidate for an importer of muropeptides.

To investigate whether YejABEF constitutes a novel PG recycling transporter in *A. tumefaciens*, we deleted the full operon corresponding to *yejABEF* (Atu0187–Atu0190) (Fig. 2C) and used UPLC to check the

supernatant of this mutant for the accumulation of PG fragments. As would be expected, anhydromuramyl tri-, tetra- and pentapeptides accumulated in large quantities in the extracellular milieu of the $\Delta yejABEF$ mutant (Fig. 2B). Since deletion of *ampD* results in the accumulation of muropeptides in the cytoplasm of *A. tumefaciens*, we reasoned that deletion of the transporter in a $\Delta ampD$ background must necessarily prevent this. We therefore checked the cytoplasmic soluble muropeptides in a $\Delta yejABEF \Delta ampD$ mutant (Fig. 2D) using UPLC. There was no cytoplasmic muropeptide accumulation in the double mutant, indicating that YejABEF is the sole transporter responsible for muropeptide recycling in *A. tumefaciens*. Further, ectopic expression of the known MFS muropeptide importer AmpG from *E. coli* restored the cytosolic accumulation of muropeptides in the $\Delta yejABEF \Delta ampD$ background (Fig. S2), confirming that these transporters have the same function. Interestingly, the profile of accumulating muropeptides with AmpG expression was altered, highlighting the different specificity of these transporters (Fig. S2): there were no dimeric muropeptides, reduced levels of tri- and pentapeptide muropeptides and no GlcNAc–MurNAc muropeptides (or their products), consistent with the known specificity of AmpG²⁴. Finally, we produced anhydro-disaccharide tetrapeptides with the non-canonical D-amino acid D-Met instead of D-Ala in the fourth position (M4N^{Met}) as a probe for PG recycling¹⁶. A $\Delta ampD$ culture

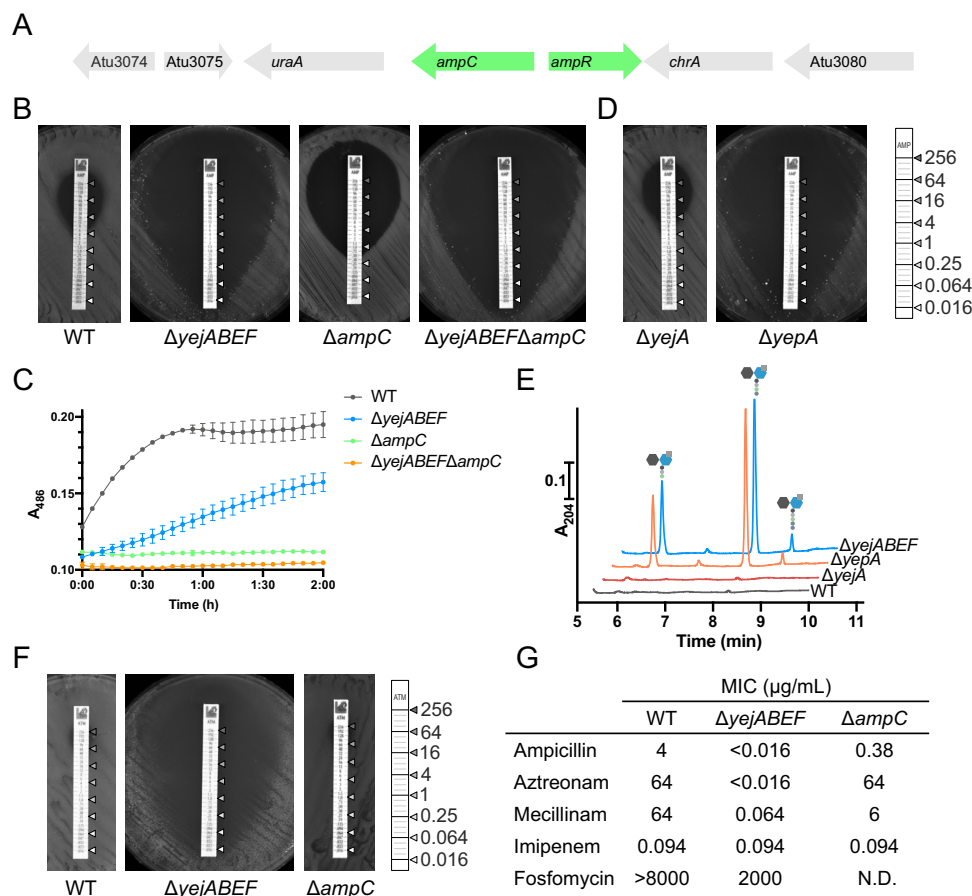


Fig. 3 | $\Delta yejABEF$ is hypersensitive to Ampicillin, in a manner only partly dependent on the β -lactamase AmpC. **A** Genomic context of the AmpC β -lactamase in *A. tumefaciens*, showing proximity to canonical AmpR repressor. **B** Comparison of Amp resistance of *A. tumefaciens* WT, $\Delta yejABEF$, $\Delta ampC$ and $\Delta yejABEF\Delta ampC$ strains by growth on LB plates with Ampicillin MIC test strips ($\mu\text{g/mL}$). **C** Hydrolysis of nitrocefin by lysates of *A. tumefaciens* WT, $\Delta yejABEF$, $\Delta ampC$ and $\Delta yejABEF\Delta ampC$ strains, measured by following A_{486} . $n = 3$ biologically independent experiments, error bars represent standard deviation from

mean. Source data are provided as a Source Data file. **D** Comparison of Amp resistance of *A. tumefaciens* $\Delta yejA$ and $\Delta yepA$ (Atu1774) strains. **E** Accumulation of mucopeptides in the supernatants of *A. tumefaciens* WT, $\Delta yejA$, $\Delta yepA$ and $\Delta yejABEF$ strains, measured by UPLC. **F** Comparison of Aztreonam resistance of *A. tumefaciens* WT, $\Delta yejABEF$ and $\Delta ampC$ strains by growth on LB plates with Aztreonam MIC test strips. **G** Minimal inhibitory concentration (MIC) values of *A. tumefaciens* WT, $\Delta yejABEF$ and $\Delta ampC$ to β -lactams Ampicillin, Aztreonam, Mecillinam, Imipenem, and MurA-inhibitor Fosfomycin.

exogenously supplemented with M4N^{Met} yielded an accumulation of anhydromurNAc-P4 $^{\text{Met}}$ (i.e. M4N^{Met} processed by NagZ) in the cytoplasm (Fig. 2E), which did not occur in the $\Delta yejABEF\Delta ampD$ mutant, further confirming the requirement of YejABEF for the import of anhydromuropeptides into the cytoplasm.

Role of PG recycling in β -lactam resistance in *A. tumefaciens*

A. tumefaciens encodes a canonical inducible AmpC β -lactamase system where the import of anhydromuropeptides controls β -lactamase expression through the regulator AmpR^{25,26} (Fig. 3A). We therefore reasoned that the $\Delta yejABEF$ mutant could show decreased Ampicillin (Amp) resistance through lower β -lactamase expression. Indeed, we observed a >250-fold decrease in Amp MIC in the transporter mutant (Fig. 3B). Consistently, hydrolysis of the chromogenic cephalosporin nitrocefin was decreased considerably in the mutant, indicating lower AmpC activity (Fig. 3C).

Interestingly, the three parts of the transporter that are required for Fosfomycin resistance form a cluster with the putative SBP YejA (Atu0187). Using RT-PCR, we confirmed that *yejA* is co-expressed with *yejBEF* on a single mRNA (Fig. S3A). As mentioned, Tn insertions in *yejA* were not significantly reduced under Fosfomycin treatment. Instead, we found that mutation of the *yejA* paralog Atu1774 conferred Fosfomycin sensitivity. To investigate the potential role of these SBPs, we generated single mutants of *yejA*

and Atu1774 and compared them with mutants of other parts of the transporter (Fig. 3C). The Amp sensitivity of the $\Delta yejB$, $\Delta yejE$, $\Delta yejF$ and $\Delta \text{Atu1774}$ mutants recapitulated that of the entire operon deletion mutant (Fig. S3B), indicating that these components are required for the PG recycling function of the transporter, while the $\Delta yejA$ mutant was phenotypically identical to the WT. Additionally, we observed the accumulation of PG fragments in the supernatant of $\Delta \text{Atu1774}$ on the same levels as for $\Delta yejABEF$, while $\Delta yejA$ again reflected the WT (Fig. 3E). Collectively these results demonstrate that Atu1774, instead of YejA, is the SBP involved in PG recycling in *A. tumefaciens*, and so we renamed it YepA for Yej-peptidoglycan binding protein A.

Remarkably, we noticed that $\Delta yejABEF$ and the single mutants $\Delta yejB$, $\Delta yejE$, $\Delta yejF$ and $\Delta yepA$ were more Amp sensitive than $\Delta ampC$ (Fig. 3B), meaning that the Amp hypersensitivity of the PG recycling defective mutants was not just a result of decreased β -lactamase activity. Indeed, the nitrocefin hydrolysis assay showed that $\Delta yejABEF$ retained more β -lactamase activity than $\Delta ampC$ despite its lower Amp resistance (Fig. 3C). This was further confirmed by testing sensitivity of both mutants to aztreonam, a monobactam β -lactam antibiotic. The $\Delta ampC$ mutant showed an identical resistance profile to the WT, suggesting that AmpC plays no role in resistance of *A. tumefaciens* to aztreonam, while $\Delta yejABEF$ was once again hypersensitive (Fig. 3F).

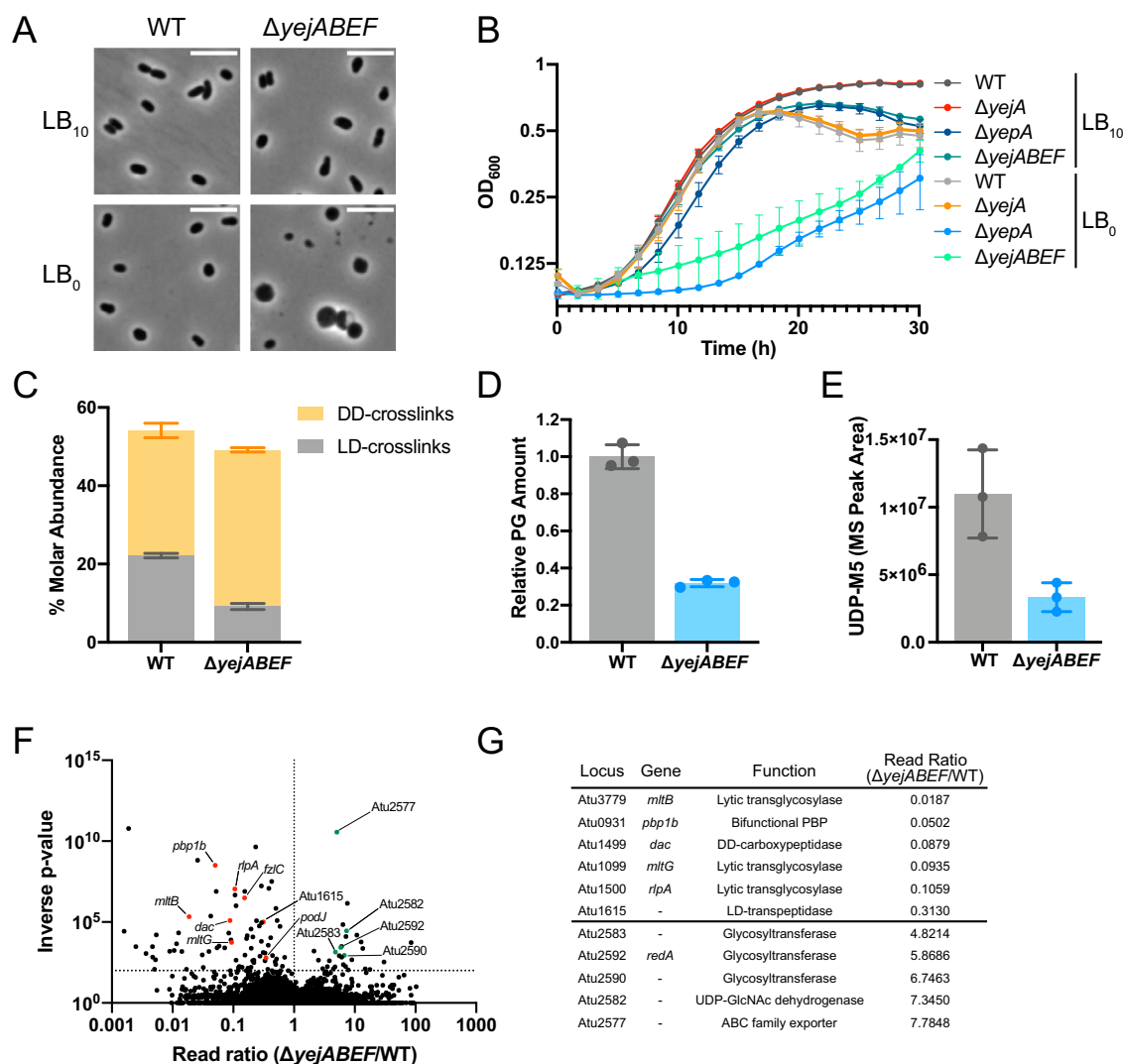


Fig. 4 | PG recycling is required for cell wall integrity in *A. tumefaciens*.

A–E Phenotypic analysis of *A. tumefaciens* WT and *ΔyejABEF* strains. **A** Phase contrast microscopy of WT and *ΔyejABEF* cells grown on LB₁₀ and LB₀. Scale bar length is 5 μm. Images are representative of three biologically independent replicates. **B** Growth curves of WT and *ΔyejABEF* on LB₁₀ and LB₀. *n* = 3 biologically independent experiments, error bars represent standard deviation from mean. **C** Molar abundance of DD- and LD-crosslinks in cell walls determined by UPLC analysis of WT and *ΔyejABEF* PG. **D** Relative PG amounts determined by total area under UPLC chromatograms of WT and *ΔyejABEF* PG. **E** LC-MS quantification of primary soluble

PG precursor UDP-M5 in WT and *ΔyejB*. **F** Volcano plot showing the ratio of Tn-Seq reads mapped to genes in the *A. tumefaciens* *ΔyejABEF* strain compared to WT as control. Selected synthetically detrimental (red) and synthetically beneficial (green) hits are highlighted. *p*⁻¹ value determined from Mann-Whitney U test (threshold *p*⁻¹ > 100). **G** Table listing selected synthetically detrimental or beneficial hits in *ΔyejABEF* Tn-Seq discussed in the main text, with annotations. Selected hits were genes putatively related PG homeostasis or cell division with significance value above threshold. Error bars in graphs represent standard deviation from mean. Source data for **B–E** are provided as a Source Data file.

PG recycling is required for cell wall integrity in *A. tumefaciens*

We therefore hypothesised that the absence of YejBEF might cause cell wall defects which result in increased sensitivity to β-lactam antibiotics. To challenge cell wall strength, we first grew the mutant and WT strains in LB with no added NaCl (LB₀) to see how growth would be affected by low-osmolarity conditions. The *ΔyejABEF* mutant displayed cell swelling and lysis (Fig. 4A) as well as a severe growth defect which indicated a compromised cell wall (Fig. 4B). As expected, *ΔyejA* but not *ΔyejB* recapitulated this phenotype (Fig. 4B) further strengthening the role of YejA as the PG SBP. To confirm that this effect was directly related to loss of PG recycling, we tested whether ectopic expression of *E. coli ampG* on a plasmid restores LB₀ growth in *ΔyejABEF* and found that it does rescue growth and morphology (Fig. S4A). To investigate this effect further, we chemically analysed the cell wall of the *ΔyejABEF* mutant and WT using UPLC (Figs. 4C, D, S5). While total crosslinking was slightly decreased in the mutant (Fig. 4C), interestingly, LD-crosslinking was considerably more affected than DD-crosslinking,

which was actually slightly higher relative to the WT. Since LD-transpeptidases are not affected by most β-lactam antibiotics¹⁷, a higher dependence of the *ΔyejABEF* mutant on PBPs for PG crosslinking could be a possible contributing factor to its decreased β-lactam tolerance. Importantly, the total amount of PG in the mutant, as determined by the area under the whole chromatogram normalised to the optical density of the culture, was decreased considerably (Fig. 4D), suggesting that PG biogenesis was compromised. Quantification of the primary soluble cytoplasmic PG precursor UDP-M5 showed a corresponding decrease (Fig. 4E), indicating that PG recycling is an important source of material for PG synthesis in *A. tumefaciens*.

To further investigate the cell wall defects of *ΔyejABEF*, we used Tn-Seq to identify genes which confer greater or reduced fitness to the mutant when interrupted by Tn insertion (Fig. 4F, G, Supplementary Data 2). Consistent with the observed defects of *ΔyejABEF* in PG synthesis and crosslinking, we found that synthetically detrimental mutants included a putative LD-transpeptidase (Atu1615), bifunctional

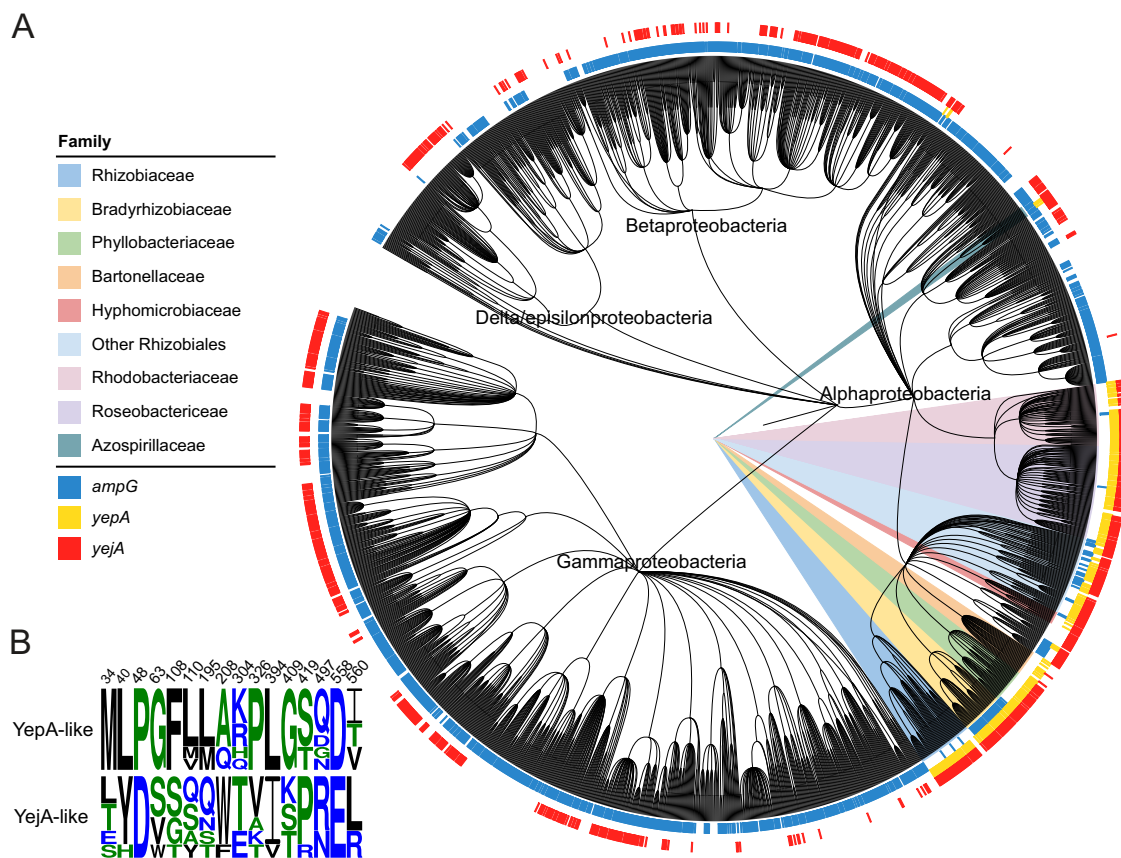


Fig. 5 | YefABEF is widespread in the proteobacteria, but YepA is only present in the Alphaproteobacteria. A Phylogenetic tree showing distribution of *ampG*, *yepA* and *yefA* in the Proteobacteria. **B** Molecular fingerprint residues of YepA used to differentiate between YefA and YepA.

PBP1b (Atu0931), DD-carboxypeptidase (Atu1499), and LTs MltB (Atu3779), MltG (Atu1099) and RlpA (Atu1500), suggesting that additive effects caused by the loss of these PG synthesis and remodelling proteins in combination with PG recycling results in loss of fitness or non-viability. Two other synthetically detrimental candidates were also related to cell division and cell wall synthesis, further linking YefBEF-YepA to envelope defects: PodJ (Atu0499) which denotes the old pole during division²⁷ and is required for chromosome segregation²⁸ and normal cell division²⁹ in *A. tumefaciens*, and the FtsZ-binding protein FzIC (Atu2824) which anchors FtsZ to the membrane in *Caulobacter crescentus* and has been linked to PG hydrolysis through synthetic lethality screens^{30,31}. These results were recapitulated by a second Tn-Seq comparing insertions in the $\Delta yepA$ and $\Delta yefA$ mutants (Fig. S4B).

Conversely, mutations in several glycosyltransferases (Atu2583, Atu2590, Atu2592), a UDP-GlcNAc dehydrogenase (Atu2582) and a putative ABC exporter (Atu2577) improved fitness of the $\Delta yefABEF$ mutant. These genes form part of a cluster likely to be involved in the synthesis of an uncharacterised glycan, previously reported to be required for resistance to phenazines in *A. tumefaciens*³². Since its synthesis seems to use UDP-GlcNAc as a building block, we hypothesised that these mutations might redirect GlcNAc flux to PG synthesis, thereby improving $\Delta yefABEF$ fitness. However, this does not seem to be the case, as measured UDP-M5 and UDP-MurNAc levels in $\Delta Atu2582$ and $\Delta Atu2582\Delta yefABEF$ strains showed no differences to their WT and $\Delta yefABEF$ counterparts (Fig. S4C). It remains to be seen what role this polymer plays in cell wall biology in *A. tumefaciens*.

YefBEF-YepA is conserved in the Rhizobiales and Rhodobacteriales orders of the Alphaproteobacteria

Finally, to define the degree of conservation of the PG recycling function of YefBEF in bacteria, we generated a molecular fingerprint

that allowed us to differentiate between YepA and YefA. Using the JDet package³³, we generated a set of specificity-determining residues from an alignment of YefA and YepA orthologs (Fig. 5B). While YefABEF is broadly conserved across the proteobacteria, YepA is exclusive to the Alphaproteobacteria (Fig. 5A), being present in almost all families in the Rhizobiales and Rhodobacteriales orders, which also mostly lack AmpG. These bacteria inhabit a broad spectrum of niches including plant symbionts and pathogens (Rhizobiales), mammalian pathogens (Brucellaceae, Bartonellaceae), soil bacteria (Azospirillaceae) and photosynthetic marine bacteria (Rhodobacteriaceae) suggesting that YefBEF-YepA is not associated with one particular lifestyle. Interestingly, while most species opt either for AmpG or YefBEF-YepA, these PG transporters seem to coexist in a number of species such as in the Bradyrhizobiaceae indicating that one or both could be used under different conditions.

Discussion

PG biosynthesis and remodelling have been the subject of decades of research, but the focus on relatively few model organisms has left the diversity of these processes poorly understood. This particularly applies to PG recycling, which has additionally suffered from a perceived lack of importance, since its interruption in the Gram-negative model organism *E. coli* has no detrimental effect to the bacterium under lab conditions⁴. Muropeptides are a unique molecular signature of bacteria which are highly immunogenic³⁴ and often mediate inter-species interactions³. Therefore, PG recycling is a factor which influences bacterial virulence and immune response activation^{35–37}. In addition, the high turnover of PG during the cell cycle means that significant amounts of material would be lost if it were not recycled. Many bacteria outside the typical models lack orthologs of key PG recycling enzymes, but have others⁴, suggesting there are alternative

enzymes or pathways to be discovered. For example, it was recently uncovered that both *Vibrio cholerae*⁴⁶ and *Acinetobacter baumannii*^{38,39} have different functional analogs of the *E. coli* LD-carboxypeptidase LdcA with a separate but convergent evolution. We noticed that many bacteria belonging to the Rhizobiales and Rhodobacterales orders of the Alphaproteobacteria lacked an AmpG transporter despite having orthologs of the other key PG recycling enzymes AmpD and NagZ. Using the plant pathogen *A. tumefaciens* as model, we identified an alternative ABC transporter that takes over this role. *A. tumefaciens* is a fascinating model to study the growth and division of bacteria, because it exhibits an unusual asymmetric polar growth mode, and relies heavily on the typically dispensable LD-transpeptidases for PG crosslinking⁴⁰.

What happens to the PG after it is transported into the cell? An interesting difference between muropeptide recycling in *A. tumefaciens* and *E. coli* is the variety of intracellular muropeptide species which accumulate in the Δ ampD mutant. In *E. coli*, only the NagZ- and LdcA-processed anhydromuramyl tripeptide accumulates on significant levels⁵, whereas in our *A. tumefaciens* Δ ampD mutant, peaks corresponding to a wide variety of anhydromuramyl tri-, tetra- and pentapeptides are present as well as dimeric muropeptides (Fig. 1B). Since direct recycling of tetrapeptide precursors is typically highly toxic to the cell^{9,16}, we suggest that *A. tumefaciens* does not directly reuse the PG peptide by ligation with UDP-MurNAc as in some other Gram-negative bacteria. Instead, it might simply degrade the released peptides and reincorporate the released amino acids into de novo precursor synthesis or use them as a source of C or N. This idea is supported by the lack of Mpl ligase or LD-carboxypeptidase orthologs in *A. tumefaciens*, and by the genetic context of *yejABEF* since it clusters with a putative D-alanine dehydrogenase *dadA* (Atu0192, labelled as a pseudogene due to a frameshift mutation, but this occurs after the catalytic domain suggesting that it could have retained its activity) and glutamine synthetase *glnA* (Atu0193) which uses glutamate as a substrate.

It is interesting that the PG SBP YepA is located separately from the rest of the transporter in the genome. This raises the possibility of separate transcriptional regulation of the “core” and PG-binding parts of the transporter, which would allow its PG recycling function to be regulated independently of its function as a broad-spectrum peptide importer. In addition, the presence of two SBPs competing for the same core could allow regulation of transporter function at the protein level, since higher levels of one SBP might be expected to preclude binding of the other. YepA also seems to have a conserved position beside a both a predicted cytoplasmic DsbA-like protein (Atu1775) of unknown function and the essential periplasmic polar growth protein RgsG⁴¹, but the function of these two genes remains to be identified.

The presence of an AmpC induction system based on released muropeptides has been previously reported in *A. tumefaciens*²⁵, but the mechanism through which muropeptides enter the cell has not been revealed until now. As a soil bacterium, *A. tumefaciens* likely encounters β -lactam antibiotics in the environment produced by competing organisms to interact or fight for their niche⁴², so the presence of an inducible β -lactamase system could be a way to counter these. However, although YejABEF does control the induction of AmpC, we showed that its effect on β -lactam sensitivity is also partly caused by cell wall defects which occur in its absence. The requirement of YejABEF for cell wall integrity and normal growth was surprising, since *E. coli* has been shown to have no physiological defects on deletion of AmpG⁴. A possible reason for this is the different ways in which these bacteria grow: while *E. coli* elongates all along the cell⁴³, *A. tumefaciens* elongates from one pole⁴⁰. Integrity of the newly synthesised PG is perhaps more susceptible to a lowered flux of material when synthesis is concentrated on a single area.

Our Tn-Seq screen in Δ yejABEF revealed synthetically lethal cell wall-related genes including a bifunctional PBP, an LD-transpeptidase,

and three LTs. Insertions in the synthetic PBP and LD-transpeptidase could result in lethality due to additive effects on top of the synthesis defects that already occur. Mutation of LTs is known to cause periplasmic stress due to periplasmic crowding caused by the accumulation of PG chains⁴⁴. Interruption of PG recycling could exacerbate periplasmic crowding, since we observed PG fragments accumulating in large amounts in the supernatant of Δ yejABEF. That we observe chains accumulating in the cytoplasm of Δ ampD but not in the supernatant of Δ yejABEF suggests they could be too large to escape the outer membrane, accumulating in the periplasm and thereby causing osmotic stress.

Our Tn-Seq screen also revealed that Tn insertions in a gene cluster likely responsible for the synthesis of an uncharacterised glycan alleviated the fitness cost of deleting Δ yejABEF. While this could be consistent with the idea of alleviating periplasmic crowding, *A. tumefaciens* also produces osmoregulated cyclic β -glucans⁴⁵, which did not show up in our screen, meaning this is likely not the case. This polymer has previously been reported as required for tolerance of the phenazine pyocyanin in *A. tumefaciens*³², suggesting it could play some role in oxidative stress metabolism. Cell wall defects have previously been associated with an overproduction of hydroxyl radicals⁴⁶, and the potential role of YejABEF in periplasmic oxidative stress is a subject for future research.

YejABEF has previously been reported as important for proper bacteroid differentiation and resistance to the plant antimicrobial peptide NCR247 in *S. meliloti*^{23,47}. Though this was thought to be due to its activity as a promiscuous peptide importer, we suggest that it actually comes from its function as a PG transporter, since AmpD is also required for NCR247 tolerance and the non-PG SBP YejA is not⁴⁷. Indeed, the bacteroids formed by *S. meliloti* Δ yejE and Δ yejF mutants display an aberrant, swollen morphology²³ indicating that PG recycling could be necessary to maintain cell wall integrity in *S. meliloti* during bacteroid differentiation. *A. tumefaciens*, along with *Brucella abortus* and *Bartonella henselae*, is an intracellular pathogen, and so “hiding” its released PG from the host could be a strategy to avoid immune detection since immune receptors for PG are located intracellularly. The presence of the transporter in many other Alphaproteobacterial species, including some which share an intracellular or host-associated niche, makes it an attractive topic for further study.

The question of why *A. tumefaciens* uses an ABC transporter to recycle PG instead of a PMF-dependent MFS transporter such as AmpG remains. The use of different energy sources could mean that PG recycling is required by *A. tumefaciens* under a specific condition where ATP is available as an energy source but membrane polarisation is affected. However, *yepA* does not seem to be limited to any one particular niche, being present in diverse plant and animal pathogens and symbionts and also environmental and marine bacteria (Fig. 5). The Rhizobiales are known to be particularly rich in ABC transporters, with 146 full ABC importers present in *Sinorhizobium meliloti*^{48,49}. One possible reason for this is that it could facilitate a common mechanism of regulation of transport. Inactivation of ABC transporters on a cellular scale has been identified previously in *Rhizobium leguminosarum* in response to sensing of global cellular nitrogen availability^{50–52} or glutathione levels⁵³, through a putatively post-translational mechanism which remains to be elucidated^{50,52}. Therefore, using an ABC transporter for PG recycling could allow the cell to coordinate the regulation of this process with the regulation of acquisition of other nutrients and energy sources, perhaps in synchronisation with the cell cycle since glutathione levels are known to fluctuate during the cell cycle in the related Alphaproteobacterium *Caulobacter crescentus*⁵⁴.

Methods

Strains and growth conditions

Strains used in this study are listed in Table S1. *A. tumefaciens* strains were grown in LB, ATGN or ATSN (prepared as ref. 55 but without the

addition of FeSO_4 to avoid precipitation as its absence did not affect growth) at 30 °C unless stated otherwise. *E. coli* strains were grown in LB at 37 °C. All *A. tumefaciens* mutants are derivatives of the *Agrobacterium fabrum* strain C58. When required, antibiotics were added to growth media: Kanamycin (50 $\mu\text{g}/\text{mL}$ *E. coli*, 300 $\mu\text{g}/\text{mL}$ *A. tumefaciens*) or Amp (100 $\mu\text{g}/\text{mL}$). Growth curves were done using a microplate reader (Eon BioTek, with the BioTek Gen5 3.09 software) to measure OD_{600} of 200 μL cultures in a 96-well microplate over 28 h at 5 min intervals. Three technical replicates of three biological replicates (i.e. separate parental cultures) were used per condition. Initial cultures were prepared by adjusting exponentially growing cultures to OD_{600} 0.01.

Construction of plasmids and mutants

Expression and allelic exchange vectors were constructed using the primers outlined in Table S2. Allelic exchange vectors for *A. tumefaciens* were constructed using isothermal assembly of flanking regions with the suicide vector pNPTS139; mutagenesis was carried out as described⁵⁶. Protein expression vectors were constructed by PCR of the region of interest with addition of restriction sites by primers, then restriction digest and ligation before transformation into *E. coli* DH5 α .

Antibiotic resistance determination

Resistance to various antibiotics was determined on agar using MIC Test Strips (Liofilchem). Exponential cultures were adjusted to OD_{600} 0.1 in PBS before being spread across an LB agar plate three times using a sterile cotton swab; the plate was rotated 60° between each spreading. The strip was applied once the plate had dried fully.

Nitrocefin hydrolysis assay

Overnight cultures of *A. tumefaciens* strains were diluted 1:3 in fresh LB with 50 $\mu\text{g}/\text{mL}$ Amp added (to induce *ampC* expression) and grown for 1 h. 1 mL of culture normalised to OD_{600} 0.4 was prepared which was pelleted and washed in 1 mL of PBS. The final pellet was then resuspended in 1 mL lysis buffer (PBS with 0.2% Triton X-100, 50 $\mu\text{g}/\text{mL}$ lysozyme, and 2 mM EDTA) and incubated on ice for 30 min to lyse the cells. 200 μL reactions were set up containing 100 μL lysate, 96 μL PBS and 4 μL 500 $\mu\text{g}/\text{mL}$ nitrocefin (Oxoid) and the reaction was followed by monitoring A_{486} for 2 h in a microplate reader (Eon Biotek) with readings every 5 min.

Soluble muropeptide analysis

To determine the presence and levels of intra- and extracellular soluble muropeptides, bacteria were grown until late exponential phase (roughly OD_{600} 0.7) in minimal media before being cooled on ice for 10 min and normalised to the same OD_{600} . Cells were then harvested by centrifugation at 10,000 $\times g$ for 2 min. The supernatant was decanted and passed through a 0.22 μm filter, then boiled for 10 min, centrifuged at maximum speed in a benchtop centrifuge for 10 min to remove precipitated proteins and concentrated 20 times in a Speed-Vac system. Meanwhile, the cell pellet was washed three times in ice-cold 0.9% NaCl, resuspended in 0.9% NaCl so that the cells are 20 times concentrated and boiled for 10 min before centrifugation at maximum speed in a benchtop centrifuge for 10 min to remove the proteins and insoluble fraction.

Detection and chemical characterisation of the soluble muropeptides was carried out using an Acquity H-Class UPLC (Waters) coupled to a Xevo G2/XS QTOF mass spectrometer. Chromatographic separation was achieved using an Acquity UPLC BEH C18 column (Waters) maintained at 45 °C. A linear gradient of 0.1% formic acid in water to 0.1% formic acid in acetonitrile was used for elution. UV detection was performed at 204 nm. The QTOF instrument was operated in positive ion mode, with data collection performed in untargeted MS^c mode. The parameters were set as follows: capillary voltage

3.0 kV, source temperature 120 °C, desolvation temperature 350 °C, sample cone voltage 40 V, cone gas flow 100 L h^{-1} and desolvation gas flow 500 L h^{-1} . Data acquisition and processing was performed using the UNIFI software (Waters). A compound library of expected muropeptides was built in UNIFI by drawing the structures in ChemSketch (<http://www.acdlabs.com>). This library was used for automated processing of the data and quantification by integration of the peaks from extracted ion chromatograms.

Peptidoglycan analysis

Peptidoglycan isolation and analysis were carried out as described previously⁵⁷. Briefly, 10 mL stationary phase cultures were normalised to the same OD_{600} , pelleted, resuspended in 5% SDS and boiled for 2 h with stirring. The obtained sacculi were washed repeatedly in water to remove the SDS before analysis; pelleting was performed by ultracentrifugation in an Optima MAX-TL benchtop ultracentrifuge at 150,000 $\times g$. The final pellet was resuspended in water and digested overnight with muramidase (80 $\mu\text{g}/\text{mL}$) before adjustment to pH 9 with addition of 0.5 M sodium borate, reduction with addition of 10 mg/mL sodium borohydride for 20 min at RT and adjustment to pH 3.5 by addition of orthophosphoric acid.

Liquid chromatography was carried out using an Acquity H-Class UPLC system (Waters) equipped with an Acquity UPLC BEH C18 column (2.1 mm \times 150 mm, 130 Å pore size and 1.7 μm particle size, Waters). Chromatographic separation was achieved using a linear gradient from 0.1% formic acid in water to 0.1% formic acid in acetonitrile. Peaks were identified using in-line LC-MS and assigning peak identities using retention time. The relative amount of each muropeptide was calculated by integrating all the peaks and dividing each peak area by the total area of the chromatogram, while the total area of the chromatogram was taken as the relative density of PG per sample and expressed relative to the WT.

M4N^{Met} incorporation experiment

M4N was prepared by digesting purified *V. cholerae* sacculi using the lytic transglycosylase MltA. An in vitro Ldt-mediated exchange reaction with purified LdtA was used to swap the D-Ala in position 4 with D-Met to produce M4N^{Met} as described⁵⁸. 10 mL of exponentially growing *A. tumefaciens* cultures was pelleted and resuspended in 200 μL fresh medium, and -15 μg M4N^{Met} was added to each. The cultures were then grown for a further hour and prepared for soluble precursor analysis as described above.

Bioinformatic analyses

Sequences of SBPs corresponding to YejA and YepA were identified in representative species spanning the Rhizobiales and Rhodobacterales orders of the Alphaproteobacteria: *A. tumefaciens* (UniProt YejA: A9CKL4, YepA: A9CIN5), *Sinorhizobium meliloti* (YejA: Q92T30, YepA: Q92PT7), *Bartonella henselae* (YepA only: A0A0H3LXD4), *Brucella melitensis* (YejA: Q8YEE4, YepA: Q8YC41), *Ochrobactrum anthropi* (YejA: A6WUU2, YepA: A6X540), *Dinoroseobacter shibae* (YejA: A8LQB5, YepA: A8LK88) and *Phaeobacter inhibens* (YejA: I7EQS1, YepA: I7EWM7). SBPs were identified by phenotype for *D. shibae* and *P. inhibens* (using FitnessBrowser⁵⁹ to look for the SBP with the expected β -lactam and Fosfomycin sensitivity phenotypes) and eggNOG 5.0⁶⁰ using fine-grained orthologs of Atu1774 and Atu0187 for the others. Sequences were aligned using MUSCLE⁶¹ and the JDet package³³ was used to find specificity-determining positions (SDPs), which were visualised using WebLogo⁶². To produce a phylogenetic tree, all YejA orthologs were downloaded from OrthoDB v10 (group 231800at1224)⁶³, aligned using MUSCLE v5 and the previously determined SDPs were used to label each as either YejA or YepA. AmpG orthologs from OrthoDB v10 (group 542870at1224) were filtered by BLASTP against *E. coli* AmpG (UniProt POAEI6) using an E value cutoff of 1×10^{-25} . PhyloT was used to produce a phylogenetic tree of all

species on OrthoDB and orthologs of YejA, YepA and AmpG were mapped against this. The final tree was visualised using iTOL⁶⁴.

RT-PCR of *yejABEF* cluster

All kits were used as per the manufacturer's instructions. Total RNA was extracted from *A. tumefaciens* C58 WT using the RNeasy Plus Mini Kit (QIAGEN), DNA was degraded using the TURBO DNA-free kit (Thermo) and cDNA was synthesised using the Maxima Reverse Transcriptase (Thermo). PCR was performed with primers FCP6349-6357 using the VeriFi polymerase (PCRIBIO), with a 64 °C annealing temperature and 1.5 min elongation time.

Transposon sequencing

For identification of conditionally essential genes, Tn-Seq was performed broadly as described elsewhere⁶⁵, adapted for *A. tumefaciens*. 3–5 × 10⁵ transposon mutants were generated per library by conjugation of *A. tumefaciens* C58 with *E. coli* SM10λ-pir carrying the mariner transposon donor plasmid pSC189⁶⁶. Mutant libraries were selected on LB plates with 500 µg/mL kanamycin (to select for the transposon), 25 µg/mL streptomycin (to remove the donor *E. coli*) and 2 mg/mL Fosfomycin where appropriate. The libraries were collected, genomic DNA extracted, and pooled genomic DNA fragments were sequenced using a MiSeq system (Illumina). Insertion sites were identified and statistical representation of transposon insertions determined using the ConArtist pipeline as described in ref. 67.

Reporting summary

Further information on research design is available in the Nature Portfolio Reporting Summary linked to this article.

Data availability

Raw sequencing reads for Tn-Seq experiments are available at the NCBI Sequence Read Archive (BioProjects [PRJNA869898](#) and [PRJNA869899](#)). Sequences for YejA and AmpG orthologs were obtained from OrthoDB v10⁶³, groups 231800at1224 for YejA and 542870at1224 for AmpG. Reference AmpG and SBP sequences were obtained from UniProt under accession codes [POAE16](#) for AmpG and as follows for SBPs: *A. tumefaciens* (YejA: [A9CKL4](#), YepA: [A9CIN5](#)), *Sinorhizobium meliloti* (YejA: [Q92T30](#), YepA: [Q92PT7](#)), *Bartonella henselae* (YepA only: [A0A0H3LXD4](#)), *Brucella melitensis* (YejA: [Q8YEE4](#), YepA: [Q8YC41](#)), *Ochrobactrum anthropi* (YejA: [A6WUU2](#), YepA: [A6X540](#)), *Dinoroseobacter shibae* (YejA: [A8LQB5](#), YepA: [A8LK88](#)) and *Phaeobacter inhibens* (YejA: [I7EQS1](#), YepA: [I7EWM7](#)). All other data generated or analysed during this study are included in this published article (and its supplementary information files). Source data are provided with this paper.

References

- Vollmer, W., Blanot, D. & De, M. A. Pedro, Peptidoglycan structure and architecture. *FEMS Microbiol. Rev.* **32**, 149–167 (2008).
- Vollmer, W., Joris, B., Charlier, P. & Foster, S. Bacterial peptidoglycan (murein) hydrolases. *FEMS Microbiol. Rev.* **32**, 259–286 (2008).
- Irazoki, O., Hernandez, S. B. & Cava, F. Peptidoglycan muropeptides: Release, perception, and functions as signaling molecules. *Front. Microbiol.* **10**, 500 (2019).
- Park, J. T. & Uehara, T. How Bacteria Consume Their Own Exoskeletons (Turnover and Recycling of Cell Wall Peptidoglycan). *Microbiol. Mol. Biol. Rev.* **72**, 211–227 (2008).
- Jacobs, C., Huang, L. J., Bartowsky, E., Normark, S. & Park, J. T. Bacterial cell wall recycling provides cytosolic muropeptides as effectors for β-lactamase induction. *EMBO J.* **13**, 4684–4694 (1994).
- Jacobs, C. et al. AmpD, essential for both β-lactamase regulation and cell wall recycling, is a novel cytosolic N-acetylmuramyl-L-alanine amidase. *Mol. Microbiol.* **15**, 553–559 (1995).
- Cheng, Q., Li, H., Merdek, K. & Park, J. T. Molecular Characterization of the β-N-Acetylglucosaminidase of *Escherichia coli* and Its Role in Cell Wall Recycling. *J. Bacteriol.* **182**, 4836–4840 (2000).
- Vötsch, W. & Templin, M. F. Characterization of a β-N-acetylglucosaminidase of *Escherichia coli* and elucidation of its role in muropeptide recycling and β-lactamase induction. *J. Biol. Chem.* **275**, 39032–39038 (2000).
- Templin, M. F., Ursinus, A. & Höltje, J. V. A defect in cell wall recycling triggers autolysis during the stationary growth phase of *Escherichia coli*. *EMBO J.* **18**, 4108–4117 (1999).
- Gisin, J., Schneider, A., Nägele, B., Borisova, M. & Mayer, C. A cell wall recycling shortcut that bypasses peptidoglycan de novo biosynthesis. *Nat. Chem. Biol.* **9**, 491–493 (2013).
- Borisova, M., Gisin, J. & Mayer, C. The N-Acetylmuramic Acid 6-Phosphate Phosphatase MupP Completes the *Pseudomonas* Peptidoglycan Recycling Pathway Leading to Intrinsic Fosfomycin Resistance. *mBio* **8**, e00092–17 (2017).
- Fumeaux, C. & Bernhardt, T. G. Identification of MupP as a new peptidoglycan recycling factor and antibiotic resistance determinant in *Pseudomonas aeruginosa*. *mBio* **8**, e00102–17 (2017).
- Mengin-Lecreux, D., Van Heijenoort, J. & Park, J. T. Identification of the *mpl* gene encoding UDP-N-acetylmuramate: L-alanyl-γ-D-glutamyl-meso-diaminopimelate ligase in *Escherichia coli* and its role in recycling of cell wall peptidoglycan. *J. Bacteriol.* **178**, 5347–5352 (1996).
- Goodell, E. W. Recycling of murein by *Escherichia coli*. *J. Bacteriol.* **163**, 305–310 (1985).
- Goodell, E. & Schwarz, U. Release of Cell Wall Peptides into Culture Medium by Exponentially Growing *Escherichia coli*. *J. Bacteriol.* **162**, 391–397 (1985).
- Hernández, S. B., Dörr, T., Waldor, M. K. & Cava, F. Modulation of Peptidoglycan Synthesis by Recycled Cell Wall Tetrapeptides. *Cell Rep.* **31**, 107578 (2020).
- Aliashkevich, A. & Cava, F. LD-transpeptidases: the great unknown among the peptidoglycan cross-linkers. *FEBS J.* **289**, 4718–4730 (2021).
- Kahan, F. M., Kahan, J. S., Cassidy, P. J. & Kropp, H. The Mechanism of Action of Fosfomycin (Phosphonomycin). *Ann. N. Y. Acad. Sci.* **235**, 364–386 (1974).
- Seweryn, P. et al. Structural insights into the bacterial carbon-phosphorus lyase machinery. *Nature* **525**, 68–72 (2015).
- White, A. K. & Metcalf, W. W. Microbial metabolism of reduced phosphorus compounds. *Annu. Rev. Microbiol.* **61**, 379–400 (2007).
- McGrath, J. W., Hammerschmidt, F. & Quinn, J. P. Biodegradation of phosphonomycin by *Rhizobium huakuii* PMY1. *Appl. Environ. Microbiol.* **64**, 356–358 (1998).
- Novikova, M. et al. The *Escherichia coli* Yej transporter is required for the uptake of translation inhibitor microcin C. *J. Bacteriol.* **189**, 8361–8365 (2007).
- Nicoud, Q. et al. *Sinorhizobium meliloti* Functions Required for Resistance to Antimicrobial NCR Peptides and Bacteroid Differentiation. *mBio* **12**, e00895–21 (2021).
- Cheng, Q. & Park, J. T. Substrate Specificity of the AmpG Permease Required for Recycling of Cell Wall Anhydro-Muropeptides. *J. Bacteriol.* **184**, 6434–6436 (2002).
- Figueroa-Cuilan, W. M. et al. Induction of AmpC-Mediated β-Lactam Resistance Requires a Single Lytic Transglycosylase in *Agrobacterium tumefaciens*. *Appl. Environ. Microbiol.* **88**, e00333–22 (2022).
- Jacobs, C., Frère, J.-M. & Normark, S. Cytosolic Intermediates for Cell Wall Biosynthesis and Degradation Control Inducible β-Lactam Resistance in Gram-Negative Bacteria. *Cell* **88**, 823–832 (1997).
- Grangeon, R., Zupan, J. R., Anderson-Furgeson, J. & Zambryski, P. C. PopZ identifies the new pole, and PodJ identifies the old pole during

- polar growth in *Agrobacterium tumefaciens*. *Proc. Natl Acad. Sci. USA* **112**, 11666–11671 (2015).
28. Robalino-Espinosa, J. S., Zupan, J. R., Chavez-Arroyo, A. & Zambryski, P. Segregation of four *Agrobacterium tumefaciens* replicons during polar growth: PopZ and PodJ control segregation of essential replicons. *Proc. Natl Acad. Sci. USA* **117**, 26366–26373 (2020).
 29. Anderson-Furgeson, J. C., Zupan, J. R., Grangeon, R. & Zambryski, P. C. Loss of PodJ in *Agrobacterium tumefaciens* Leads to Ectopic Polar Growth, Branching, and Reduced Cell Division. *J. Bacteriol.* **198**, 1883–1891 (2016).
 30. Goley, E. D., Dye, N. A., Werner, J. N., Gitai, Z. & Shapiro, L. Imaging-based identification of a critical regulator of FtsZ protofilament curvature in *Caulobacter*. *Mol. Cell* **39**, 975–987 (2010).
 31. Meier, E. L., Razavi, S., Inoue, T. & Goley, E. D. A novel membrane anchor for FtsZ is linked to cell wall hydrolysis in *Caulobacter crescentus*. *Mol. Microbiol.* **101**, 265–280 (2016).
 32. Perry, E. K. & Newman, D. K. The transcription factors ActR and SoxR differentially affect the phenazine tolerance of *Agrobacterium tumefaciens*. *Mol. Microbiol.* **112**, 199–218 (2019).
 33. Muth, T. et al. JDet: Interactive calculation and visualization of function-related conservation patterns in multiple sequence alignments and structures. *Bioinformatics* **28**, 584–586 (2012).
 34. Boneca, I. G. The role of peptidoglycan in pathogenesis. *Curr. Opin. Microbiol.* **8**, 46–53 (2005).
 35. Schaub, R. E. & Dillard, J. P. The Pathogenic Neisseria Use a Streamlined Set of Peptidoglycan Degradation Proteins for Peptidoglycan Remodeling, Recycling, and Toxic Fragment Release. *Front. Microbiol.* **10**, 73 (2019).
 36. Rosenthal, R. S., Nogami, W., Cookson, B. T., Goldman, W. E. & Folkner, W. J. Major fragment of soluble peptidoglycan released from growing *Bordetella pertussis* is tracheal cytotoxin. *Infect. Immun.* **55**, 2117–2120 (1987).
 37. Mattoo, S. & Cherry, J. D. Molecular Pathogenesis, Epidemiology, and Clinical Manifestations of Respiratory Infections Due to *Bordetella pertussis* and Other *Bordetella* Subspecies. *Clin. Microbiol. Rev.* **18**, 326–382 (2005).
 38. Dai, Y. et al. A New Class of Cell Wall-Recycling L,D-Carboxypeptidase Determines β -Lactam Susceptibility and Morphogenesis in *Acinetobacter baumannii*. *mBio* **12**, e0278621 (2021).
 39. Simpson, B. W. et al. *Acinetobacter baumannii* Can Survive with an Outer Membrane Lacking Lipooligosaccharide Due to Structural Support from Elongasome Peptidoglycan Synthesis. *mBio* **12**, e0309921 (2021).
 40. Brown, P. J. B. et al. Polar growth in the Alphaproteobacterial order Rhizobiales. *Proc. Natl Acad. Sci. USA* **109**, 1697–1701 (2012).
 41. Krol, E. et al. Tol-Pal System and Rgs Proteins Interact to Promote Unipolar Growth and Cell Division in *Sinorhizobium meliloti*. *mBio* **11**, e00306–e00320 (2020).
 42. Abrudan, M. I. et al. Socially mediated induction and suppression of antibiosis during bacterial coexistence. *Proc. Natl Acad. Sci. USA* **112**, 11054–11059 (2015).
 43. Kuru, E. et al. In Situ Probing of Newly Synthesized Peptidoglycan in Live Bacteria with Fluorescent D-Amino Acids. *Angew. Chem. Int. Ed.* **51**, 12519–12523 (2012).
 44. Weaver, A. I. et al. Lytic transglycosylases mitigate periplasmic crowding by degrading soluble cell wall turnover products. *Elife* **11**, e73178 (2022).
 45. Breedveld, M. W. & Miller, K. J. Cyclic beta-glucans of members of the family Rhizobiaceae. *Microbiol. Rev.* **58**, 145–161 (1994).
 46. Giacomucci, S., Alvarez, L., Rodrigues, C. D. A., Cava, F. & Paradis-Bleau, C. Hydroxyl Radical Overproduction in the Envelope: an Achilles' Heel in Peptidoglycan Synthesis. *Microbiol. Spectr.* **10**, e0120321 (2022).
 47. Arnold, M. F. F. et al. Genome-Wide Sensitivity Analysis of the Microsymbiont *Sinorhizobium meliloti* to Symbiotically Important, Defensin-Like Host Peptides. *mBio* **8**, e01060–17 (2017).
 48. Mauchline, T. H. et al. Mapping the *Sinorhizobium meliloti* 1021 solute-binding protein-dependent transportome. *Proc. Natl Acad. Sci.* **103**, 17933–17938 (2006).
 49. Young, J. P. W. et al. The genome of *Rhizobium leguminosarum* has recognizable core and accessory components. *Genome Biol.* **7**, R34 (2006).
 50. Prell, J. et al. The PTSNtr system globally regulates ATP-dependent transporters in *Rhizobium leguminosarum*. *Mol. Microbiol.* **84**, 117–129 (2012).
 51. Untiet, V. et al. ABC transport is inactivated by the PTS(Ntr) under potassium limitation in *Rhizobium leguminosarum* 3841. *PLoS ONE* **8**, e64682 (2013).
 52. Mulley, G. et al. Mutation of GOGAT prevents pea bacteroid formation and N₂ fixation by globally downregulating transport of organic nitrogen sources. *Mol. Microbiol.* **80**, 149–167 (2011).
 53. Cheng, G., Karunakaran, R., East, A. K., Munoz-Azcarate, O. & Poole, P. S. Glutathione affects the transport activity of *Rhizobium leguminosarum* 3841 and is essential for efficient nodulation. *FEMS Microbiol. Lett.* **364**, fnx045 (2017).
 54. Hartl, J. et al. Untargeted metabolomics links glutathione to bacterial cell cycle progression. *Nat. Metab.* **2**, 153–166 (2020).
 55. Morton, E. R. & Fuqua, C. Laboratory Maintenance of *Agrobacterium*. *Curr. Protoc. Microbiol.* **24**, 3D.1.1–3D.1.6 (2012).
 56. Morton, E. R. & Fuqua, C. Genetic manipulation of *Agrobacterium*. *Curr. Protoc. Microbiol.* **25**, 3D.2.1–3D.2.15 (2012).
 57. Alvarez, L., Hernandez, S. B., De Pedro, M. A. & Cava, F. Ultra-Sensitive, High-Resolution Liquid Chromatography Methods for the High-Throughput Quantitative Analysis of Bacterial Cell Wall Chemistry and Structure. *Methods Mol Biol.* **1440**, 11–27 (2016).
 58. Cava, F., De Pedro, M. A., Lam, H., Davis, B. M. & Waldor, M. K. Distinct pathways for modification of the bacterial cell wall by non-canonical D-amino acids. *EMBO J.* **30**, 3442–3453 (2011).
 59. Price, M. N. et al. Mutant phenotypes for thousands of bacterial genes of unknown function. *Nature* **557**, 503–509 (2018).
 60. Huerta-Cepas, J. et al. eggNOG 5.0: a hierarchical, functionally and phylogenetically annotated orthology resource based on 5090 organisms and 2502 viruses. *Nucleic Acids Res.* **47**, D309–D314 (2019).
 61. Edgar, R. C. MUSCLE: multiple sequence alignment with high accuracy and high throughput. *Nucleic Acids Res.* **32**, 1792–1797 (2004).
 62. Crooks, G. E., Hon, G., Chandonia, J.-M. & Brenner, S. E. WebLogo: a sequence logo generator. *Genome Res.* **14**, 1188–1190 (2004).
 63. Kriventseva, E. V. et al. OrthoDB v10: sampling the diversity of animal, plant, fungal, protist, bacterial and viral genomes for evolutionary and functional annotations of orthologs. *Nucleic Acids Res.* **47**, D807–D811 (2019).
 64. Letunic, I. & Bork, P. Interactive Tree Of Life (iTOL) v5: an online tool for phylogenetic tree display and annotation. *Nucleic Acids Res.* **49**, W293–W296 (2021).
 65. Chao, M. C. et al. High-resolution definition of the *Vibrio cholerae* essential gene set with hidden Markov model-based analyses of transposon-insertion sequencing data. *Nucleic Acids Res.* **41**, 9033–9048 (2013).
 66. Chiang, S. L. & Rubin, E. J. Construction of a mariner-based transposon for epitope-tagging and genomic targeting. *Gene* **296**, 179–185 (2002).
 67. Pritchard, J. R. et al. ARTIST: High-Resolution Genome-Wide Assessment of Fitness Using Transposon-Insertion Sequencing. *PLoS Genet.* **10**, e1004782 (2014).

Acknowledgements

We thank all members of the Cava lab for helpful comments and suggestions. We are grateful to Aysha Chowdury for technical assistance in construction of the Δ Atu2582 and Δ Atu2582 Δ yejABEF mutants. Research in the Cava lab is supported by the Swedish Research Council, the Laboratory for Molecular Infection Medicine Sweden (MIMS), Umeå University, the Knut and Alice Wallenberg Foundation (KAW) and the Kempe Foundation.

Author contributions

M.C.G. and F.C. conceived the study, designed the experiments, interpreted the data and wrote the paper. M.C.G. performed experiments.

Funding

Open access funding provided by Umea University.

Competing interests

The authors declare no competing interests.

Additional information

Supplementary information The online version contains supplementary material available at <https://doi.org/10.1038/s41467-022-35607-5>.

Correspondence and requests for materials should be addressed to Felipe Cava.

Peer review information *Nature Communications* thanks Christoph Mayer and the other, anonymous, reviewers for their contribution to the peer review of this work. Peer reviewer reports are available.

Reprints and permissions information is available at <http://www.nature.com/reprints>

Publisher's note Springer Nature remains neutral with regard to jurisdictional claims in published maps and institutional affiliations.

Open Access This article is licensed under a Creative Commons Attribution 4.0 International License, which permits use, sharing, adaptation, distribution and reproduction in any medium or format, as long as you give appropriate credit to the original author(s) and the source, provide a link to the Creative Commons license, and indicate if changes were made. The images or other third party material in this article are included in the article's Creative Commons license, unless indicated otherwise in a credit line to the material. If material is not included in the article's Creative Commons license and your intended use is not permitted by statutory regulation or exceeds the permitted use, you will need to obtain permission directly from the copyright holder. To view a copy of this license, visit <http://creativecommons.org/licenses/by/4.0/>.

© The Author(s) 2022